


Mpemba effect for a Brownian particle trapped in a single well potentialApurba Biswas^{*} and R. Rajesh[†]*The Institute of Mathematical Sciences, C.I.T. Campus, Taramani, Chennai 600113, India
and Homi Bhabha National Institute, Training School Complex, Anushakti Nagar, Mumbai 400094, India* (Received 2 May 2023; accepted 3 August 2023; published 17 August 2023)

The Mpemba effect refers to the counterintuitive phenomenon of a hotter system equilibrating faster than a colder system when both are quenched to the same low temperature. For a Brownian particle trapped in a piecewise linear single well potential that is devoid of any other metastable minima, we show the existence of the Mpemba effect for a wide range of parameters through an exact solution. This result challenges the prevalent explanation of the Mpemba effect that requires the energy landscape to be rugged with multiple minima. We also demonstrate the existence of inverse and strong Mpemba effects.

DOI: [10.1103/PhysRevE.108.024131](https://doi.org/10.1103/PhysRevE.108.024131)**I. INTRODUCTION**

The Mpemba effect describes an anomalous relaxation phenomenon wherein a system that is initially hotter equilibrates faster than a system that is initially cooler, when both systems are quenched to the same low temperature [1]. Recently, there has been considerable experimental and theoretical interest in the Mpemba effect. The effect was first observed in the freezing of water [1–9], though its existence in water is still debated [10]. However, it has now been experimentally observed in a wide range of physical systems such as magnetic alloys [11], polylactides [12], clathrate hydrates [13], colloidal systems [14–17], etc. Theoretical studies, focusing on model systems, have shown the existence of the Mpemba effect in spin systems [18–23], Markovian systems with few states [24,25], particles diffusing in a potential [26–30], active systems [31], spin glasses [32], molecular gases in contact with a thermal reservoir [33–36], quantum systems [37–39], systems with phase transitions [21,40–42], and granular systems [43–50]. A recent theoretical investigation employing a geometric approach to understanding such an anomalous relaxation is presented in Ref. [51].

Several system-specific reasons have been proposed to explain the Mpemba effect. For example, the different reasons proposed for the Mpemba effect in water include evaporation [2], convection [3], dissolved gases [4], supercooling [5], hydrogen bonding [6–8], and nonequipartition of energy [9]. For clathrate hydrates [13], the interplay between evaporation and the properties of hydrogen bonds has been suggested, while the Mpemba effect in magnetic alloys [11] has been attributed to the kinetic arrest of nonequilibrium phase during the relaxation. However, a general understanding of the origin of the Mpemba effect is lacking. Recently, insights obtained from theoretical studies, in particular analytically tractable models with only a few degrees of freedom, suggest that

the main driver of the Mpemba effect is the ruggedness or the presence of multiple minima in the energy landscape. In particular, it has been suggested that a metastable minimum, in addition to the global minimum, tends to trap a system at lower temperature more effectively than a system at higher temperature, resulting in a faster relaxation of the hotter system [18,19,24,26,31,52]. This viewpoint was further supported in a recent experiment on a single Brownian particle diffusing in an asymmetric double well harmonic potential with linear slopes near the boundaries of the domain, where the Mpemba effect was clearly demonstrated [14]. However, the necessity of a metastable minimum for the Mpemba effect has been questioned in recent works [26,52]. For a particular choice of a piecewise constant potential, it was shown that the Mpemba effect is observed when the metastable state has neutral equilibrium [26], while its existence was shown for the particular case of a double well potential when the metastability is just lifted [52].

In this paper, we solve exactly for the relaxation dynamics of a Brownian particle in a piecewise linear single well potential. By obtaining the phase diagram for different combinations of the parameters defining the potential, we show that the Mpemba effect is observable for a wide choice of potentials, conclusively showing that the origin of the Mpemba effect does not require the energy landscape to have metastable minima, in addition to the global minimum. We also demonstrate the existence of the inverse Mpemba effect for systems that are heated, as well as the strong Mpemba effect when a colder system cools exponentially faster. In addition, we show numerically the presence of the Mpemba effect for an overdamped particle in a single well asymmetric harmonic potential that can be realized in an experimental setup similar to that of Ref. [14].

II. MODEL AND FORMALISM

We consider a Brownian particle in one dimension trapped in a single well potential $\tilde{U}(\tilde{x})$ that is infinite outside a domain of length L . The thermal environment is

*apurbab@imsc.res.in

†rrajesh@imsc.res.in

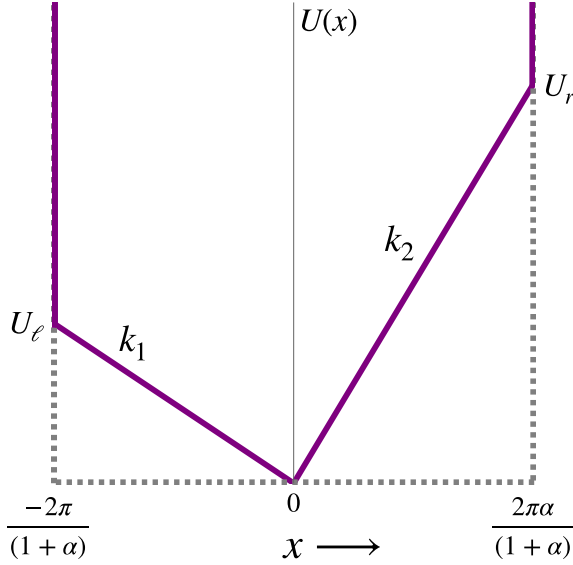


FIG. 1. Schematic diagram of the piecewise linear single well potential. The parameters k_1 and k_2 refer to the slopes, α denotes the ratio of width of the right domain to the left domain, and U_ℓ and U_r are the values of the potential at the boundaries.

characterized by noise η that has the characteristics $\langle \eta(\tilde{t}) \rangle = 0$ and $\langle \eta(\tilde{t})\eta(\tilde{t}') \rangle = 2\gamma k_B \tilde{T}_b \delta(\tilde{t} - \tilde{t}')$, where γ is the damping coefficient, \tilde{t} is time, \tilde{T}_b is the temperature of the thermal bath, and k_B is Boltzmann's constant. The motion of the particle is described by the Langevin equation

$$\gamma \frac{d\tilde{x}}{d\tilde{t}} = -\frac{d\tilde{U}}{d\tilde{x}} + \eta(\tilde{t}). \quad (1)$$

We consider dimensionless variables $x = (2\pi/L)\tilde{x}$, $T = \tilde{T}/\tilde{T}_b$, $U = \tilde{U}/(k_B\tilde{T}_b)$, and $t = (4\pi^2 k_B \tilde{T}_b / \gamma L^2)\tilde{t}$. The corresponding Fokker-Planck (FP) equation for the evolution of the probability density $p(x, t)$ in the nondimensionalized variables is given by [53,54]

$$\frac{\partial p(x, t)}{\partial t} = \frac{\partial}{\partial x} \left[\frac{dU(x)}{dx} p(x, t) \right] + \frac{\partial^2 p(x, t)}{\partial x^2} = \mathcal{L}_{\text{FP}} p(x, t), \quad (2)$$

where \mathcal{L}_{FP} is the FP operator:

$$\mathcal{L}_{\text{FP}} = \partial_x U' + \partial_x^2. \quad (3)$$

The corresponding probability current/flux in Eq. (2) is given by

$$J(x) = -\left[\frac{dU}{dx} + \frac{\partial}{\partial x} \right] p = -e^{-U(x)} \frac{d}{dx} [e^{U(x)} p]. \quad (4)$$

With the aim to demonstrate and characterize the Mpemba effect in the absence of metastable states, we consider a single well potential that is piecewise linear, as shown in Fig. 1, and is given by

$$U(x) = \begin{cases} U_\ell + k_1(x - x_{\min}), & x_{\min} < x < 0, \\ k_2 x, & 0 < x < x_{\max}, \end{cases} \quad (5)$$

where $x_{\min} = -2\pi/(1+\alpha)$ and $x_{\max} = 2\pi\alpha/(1+\alpha)$ are the positions of the boundaries, k_1, k_2 are the slopes, and U_ℓ, U_r

are the values of the potential at the boundaries. The minimum of the potential, set equal to zero, is fixed at $x = 0$. The parameter α is the ratio of the length of the right domain to that to the left domain. The motivation for the choice of x_{\min} and x_{\max} in the current form is to ensure that the introduction of asymmetry in the left and right domain lengths does not change the total length of the potential domain, which is kept fixed at 2π in the dimensionless variable. It simplifies the analysis by not taking into account an extra parameter (in the form of the total length of the potential domain) in the study of the Mpemba effect. The parameters U_ℓ, U_r , and α are the sole parameters that characterize the configuration of the potential. The piecewise linearity makes the problem analytically tractable.

To solve the FP equation in Eq. (2), we closely follow the known methods in Refs. [53,54] and the solution in Ref. [52]. We first transform the associated FP operator \mathcal{L}_{FP} to a self-adjoint operator \mathcal{L} :

$$\mathcal{L} = e^{U(x)/2} \mathcal{L}_{\text{FP}} e^{-U(x)/2} = \frac{\partial^2}{\partial x^2} - \frac{1}{4} \left(\frac{dU}{dx} \right)^2 + \frac{1}{2} \frac{d^2 U}{dx^2}. \quad (6)$$

The problem then reduces to solving the eigenvalue equation

$$\mathcal{L} \psi_n = -|\lambda_n| \psi_n, \quad (7)$$

where ψ_n are the eigenfunctions of the operator \mathcal{L} corresponding to the eigenvalue λ_n . Note that both the operators \mathcal{L} and \mathcal{L}_{FP} have the same eigenvalue λ_n , but their respective eigenfunctions $\psi_n(x)$ and $\phi_n(x)$ are related by

$$\psi_n(x) = e^{\frac{U(x)}{2}} \phi_n(x). \quad (8)$$

Given the initial probability condition $p(x', 0)$, the probability distribution function $p(x, t)$ can be obtained as

$$p(x, t) = \int W(x, t|x', 0) p(x', 0) dx', \quad (9)$$

where the transition probability or the propagator $W(x, t|x', 0)$ of the Fokker-Planck equation can be written in terms of the eigenfunctions and eigenvalues (see [53]),

$$\begin{aligned} W(x, t|x', 0) &= e^{\mathcal{L}_{\text{FP}} t} \delta(x - x') \\ &= e^{-\frac{U(x)}{2} + \frac{U(x')}{2}} \sum_n e^{\lambda_n t} \psi_n(x) \psi_n^*(x'). \end{aligned} \quad (10)$$

Substituting the transition probability into Eq. (9), one finds

$$p(x, t) = \int dx' e^{-\frac{U(x)}{2} + \frac{U(x')}{2}} \sum_n e^{\lambda_n t} \psi_n(x) \psi_n^*(x') p(x', 0). \quad (11)$$

Since $\lambda_1 = 0$, we can rewrite Eq. (11) as follows:

$$p(x, t) = \frac{e^{-U(x)}}{\mathcal{Z}(1)} + \sum_{n \geq 2} a_n e^{-\frac{U(x)}{2}} \psi_n(x) e^{-|\lambda_n| t}, \quad (12)$$

where the coefficients a_n are fixed by the initial distribution $p(x', 0)$: $a_n = \int dx' p(x', 0) e^{\frac{U(x')}{2}} \psi_n^*(x')$. The first term on the right-hand side of Eq. (12) corresponds to the eigenvalue

$\lambda_1 = 0$ and describes the final equilibrium Boltzmann distribution with partition function $\mathcal{Z}(1) = \int e^{-U(x)} dx$ at the bath temperature $T_b = 1$. The eigenvalues λ_n of the FP operator follow the order $\lambda_1 = 0 > \lambda_2 > \lambda_3 \dots$. The nondegeneracy of the eigenvalues is guaranteed as the FP operator with its boundary conditions (as discussed in Sec. II A) forms a one-dimensional regular Sturm-Liouville problem [55]. As a result, we can approximate for $p(x, t)$ at large times as

$$p(x, t) \simeq \frac{e^{-U(x)}}{\mathcal{Z}(1)} + a_2 e^{-\frac{U(x)}{2}} \psi_2(x) e^{-|\lambda_2|t}, \quad t \gg \frac{1}{|\lambda_3|}. \quad (13)$$

A. Jump conditions

Here, we outline the various jump discontinuities and boundary conditions that the probability density $p(x, t)$ should satisfy for the piecewise linear potential that is considered in this paper. The potential in Eq. (5) is not differentiable at $x = 0$, and it diverges at the boundaries $x = x_{\min}$ and x_{\max} . Let x_- and x_+ denote the points just to the left and right of the boundary of a linear segment. For the choice of potential, $U(x_+) = U(x_-)$ while $U'(x_+) \neq U'(x_-)$. Across a boundary, both probability currents are equal, i.e., $J(x_+, t) = J(x_-, t)$, and the probabilities are equal. Thus, from Eq. (4), we obtain

$$\begin{aligned} -U'(x_+)p(x_+, t) - \frac{\partial p(x_+, t)}{\partial x} \\ = -U'(x_-)p(x_-, t) - \frac{\partial p(x_-, t)}{\partial x}, \end{aligned} \quad (14)$$

$$p(x_+, t) = p(x_-, t). \quad (15)$$

The jump conditions in Eqs. (14) and (15) are satisfied by each of the eigenfunctions, and hence, using Eq. (11), as

$$\psi_n'(x_+) + \frac{U'(x_+)\psi_n(x_+)}{2} = \psi_n'(x_-) + \frac{U'(x_-)\psi_n(x_-)}{2}, \quad (16)$$

$$\psi_n(x_+) = \psi_n(x_-). \quad (17)$$

At the boundaries, the potential diverges. This implies that the probability current must vanish and it leads to the following condition in terms of the eigenfunctions:

$$\psi_n'(x) + \frac{U'(x)}{2}\psi_n(x) = 0 \quad \text{at } x = x_{\min}, x_{\max}. \quad (18)$$

The jump conditions [Eqs. (17), (16), and (18)] are utilized to solve the eigenspectrum of the Fokker-Planck operator \mathcal{L} [see Eq. (7)] as discussed in Sec. II B.

B. Eigenspectrum analysis

Now having known the necessary jump discontinuities and boundary conditions, we need to solve the following eigenvalue problem for the Fokker-Planck operator:

$$\mathcal{L}\psi_n = -|\lambda_n|\psi_n, \quad (19)$$

where ψ_n are the eigenfunctions of the self-adjoint Fokker-Planck operator \mathcal{L} [see Eq. (6)] corresponding to the eigenvalue λ_n . We solve separately in each of the two domains

of the potential $U(x)$, characterized by slopes k_1 and k_2 . This will lead to four constants of integration that will be determined by the jump conditions at the boundaries of the regions, leading to a transcendental equation for the eigenvalue. In the following, we solve for the eigenfunctions separately for the left and right domains.

1. Region I: $x_{\min} < x < 0$

Here, $U'(x) = k_1$. Then, Eq. (19) takes the form

$$\frac{d^2 \psi_n^I}{dx^2} + \left(\lambda_n - \frac{k_1^2}{4} \right) \psi_n^I = 0, \quad (20)$$

which has the solution

$$\psi_n^I(x) = A_n \sin(m_{1n}x) + B_n \cos(m_{1n}x), \quad (21)$$

where A_n, B_n are constants, and

$$m_{1n} = \sqrt{\lambda_n - \frac{k_1^2}{4}}. \quad (22)$$

The solution for the eigenfunction in the other regime is similar, but with different constants.

2. Region II: $0 < x < x_{\max}$

Here, $U'(x) = k_2$, and Eq. (19) takes the form

$$\psi_n^{II}(x) = C_n \sin(m_{2n}x) + D_n \cos(m_{2n}x), \quad (23)$$

where

$$m_{2n} = \sqrt{\lambda_n - \frac{k_2^2}{4}}. \quad (24)$$

C. Matching and boundary conditions

We now determine the different constants using the matching and boundary conditions. First, we employ the boundary conditions [see Eq. (18)] where the divergence of the potential at the boundaries leads to vanishing probability current. Next, we use the matching conditions [see Eqs. (16) and (17)] at $x = 0$, the boundary between the left and right domains, arising from the continuity of the probability current.

1. Boundary condition at x_{\min}

Since there is an infinite jump in potential at $x = x_{\min}$, the boundary condition in terms of eigenfunctions ψ_n is given by

$$\psi_n^{II}(x_{\min}) + \frac{U'(x_{\min})}{2}\psi_n^I(x_{\min}) = 0. \quad (25)$$

Substituting for ψ_n^I from Eq. (21), we obtain

$$A_n = -v_{1n}B_n, \quad (26)$$

$$v_{1n} = \frac{\frac{k_1}{2} \cos(m_{1n}x_{\min}) - m_{1n} \sin(m_{1n}x_{\min})}{\frac{k_1}{2} \sin(m_{1n}x_{\min}) + m_{1n} \cos(m_{1n}x_{\min})}. \quad (27)$$

Thus,

$$\psi_n^I(x) = B_n [\cos(m_{1n}x) - v_{1n} \sin(m_{1n}x)]. \quad (28)$$

2. Boundary condition at x_{\max}

Since there is an infinite jump in potential at $x = x_{\max}$, the boundary condition in terms of eigenfunctions ψ_n is given by

$$\psi_n'''(x_{\max}) + \frac{U_2'(x_{\max})}{2} \psi_n''(x_{\max}) = 0. \quad (29)$$

Substituting for ψ_n'' from Eq. (23), we obtain

$$C_n = -v_{2n} D_n, \quad (30)$$

$$v_{2n} = \frac{\frac{k_2}{2} \cos(m_{2n} x_{\max}) - m_{2n} \sin(m_{2n} x_{\max})}{\frac{k_2}{2} \sin(m_{2n} x_{\max}) + m_{2n} \cos(m_{2n} x_{\max})}. \quad (31)$$

Thus,

$$\psi_n''(x) = C_n [\cos(m_{2n} x) - v_{2n} \sin(m_{2n} x)]. \quad (32)$$

3. Matching condition at $x = 0$

Here, we use the jump conditions obtained from the continuity of the probability current [see Eqs. (16) and (17)] at $x = 0$. Upon simplifying, we obtain

$$B_n = D_n. \quad (33)$$

$$m_{1n} A_n + \frac{k_1}{2} D_n = m_{2n} C_n + \frac{k_2}{2} D_n. \quad (34)$$

Using Eqs. (30), (26), and (33) in Eq. (34) leads to the following transcendental equation:

$$m_{1n} v_{1n} - \frac{k_1}{2} = m_{2n} v_{2n} - \frac{k_2}{2} \quad (35)$$

in λ_n as m_{1n} and m_{2n} can be expressed in terms of λ_n [see Eqs. (22) and (24)]. Thus, solving for the eigenvalues λ_n in turn helps to find the constants A_n , B_n , C_n , and D_n .

III. MPEMBA EFFECT

We will now use Eq. (13), which describes the relaxation dynamics at late times, to quantitatively define the Mpemba effect for this system. Consider two systems P and Q initially in equilibrium at temperatures T_h and T_c , respectively, where $T_h > T_c$. Let $\pi(T)$ denote the corresponding equilibrium probability distribution at temperature T . Both systems are then simultaneously quenched to a common bath temperature $T_b = 1$ where $T_h > T_c > 1$. If P equilibrates faster than Q , the Mpemba effect is said to exist. Faster equilibration is quantified in terms of a distance from equilibrium function $D[p(t), \pi(1)]$ which measures the distance between the instantaneous distribution $p(x, t)$ from the final equilibrium Boltzmann distribution, $\pi(1)$. It has been argued [24] that the existence of the Mpemba effect is independent of the choice of $D[p(t), \pi(1)]$ provided that the distance measure obeys certain properties. These are as follows: (i) If $T_h > T_c > 1$, then the distance function should satisfy $D[\pi(T_h), \pi(1)] > D[\pi(T_c), \pi(1)]$, i.e., the higher the temperature, the larger the distance; (ii) $D[p(t), \pi(1)]$ should be a nonincreasing function of time; and (iii) $D[p(t), \pi(1)]$ should be a convex function of $p(t)$.

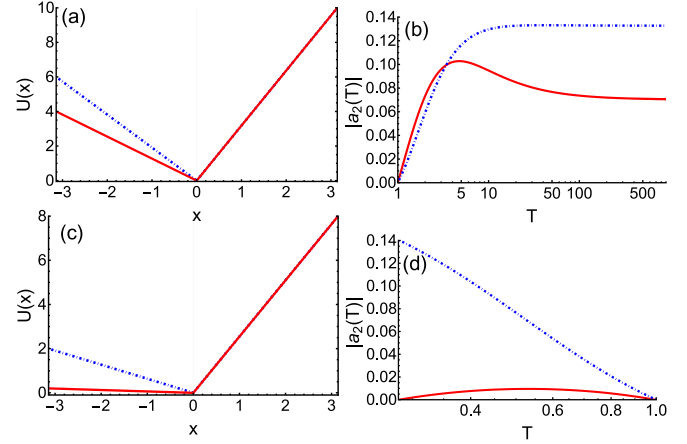


FIG. 2. Illustration of the Mpemba effect and the inverse Mpemba effect for particular choices of the potential $U(x)$. (a) Two choices of the potential corresponding to $U_\ell = 4.0$ (solid red) and $U_\ell = 6.0$ (dashed blue), keeping $U_r = 10.0$, $\alpha = 1.0$ fixed. (b) For $U(x)$ in (a) with a smaller (larger) value of U_ℓ , $|a_2(T)|$ is nonmonotonic (monotonic) for $T > 1$, demonstrating the presence (absence) of the Mpemba effect. (c) Two choices of the potential corresponding to $U_\ell = 0.2$ (solid red) and $U_\ell = 2.0$ (dashed blue) keeping $U_r = 8.0$, $\alpha = 1.0$ fixed. (d) For $U(x)$ in (c) with a smaller (larger) value of U_ℓ , $|a_2(T)|$ is nonmonotonic (monotonic) for $T < 1$, demonstrating the presence (absence) of the inverse Mpemba effect.

A convenient choice of such a distance measure is the total variation distance defined as $D[p(t), \pi(1)] \equiv L_1(t) = \int dx |p(x, t) - \pi(x, 1)|$. When $t = 0$, since $T_h > T_c$, initially $L_1^h > L_1^c$. For the Mpemba effect to exist, we require that $L_1^h < L_1^c$ at late times. In Eq. (13), since λ_2 is independent of the initial condition, the above condition for the Mpemba effect reduces to $|a_2^c| > |a_2^h|$ [19,24]. Equivalently, if $|a_2(T)|$ is nonmonotonic with temperature, then we would always be able to make a choice of T_h and T_c such that $|a_2^c| > |a_2^h|$. In Sec. IV, by considering one other distance measure, namely Kullback-Leibler divergence along with the L_1 norm, we will illustrate through an example that the Mpemba effect is independent of the choice of distance measures.

The methodology we employ is as follows. Given a potential, we solve for the eigenspectrum, which in turn allows us to compute the time evolution of the probability distribution of the particle during equilibration using Eq. (12). We then determine $|a_2(T)|$ for $T > 1$ and check for nonmonotonicity. A similar analysis can be done for the inverse Mpemba effect in which the systems are quenched to a temperature that is higher than the initial temperatures. To check for the presence of the inverse Mpemba effect, we check whether $|a_2(T)|$ for $T < 1$ is nonmonotonic.

We first show the existence of the Mpemba effect and the inverse Mpemba effect for a single well potential in order to demonstrate that the origin of the effect does not require more than one energy minima. For this purpose, we make specific choices of the single well potential, as shown in Fig. 2. For the two instances of $U(x)$, shown in Fig. 2(a), $|a_2(T)|$ for $T > 1$ is nonmonotonic for one and monotonic for the other, showing the presence and absence of the Mpemba effect depending on the choice of potential. A similar construction is possible for

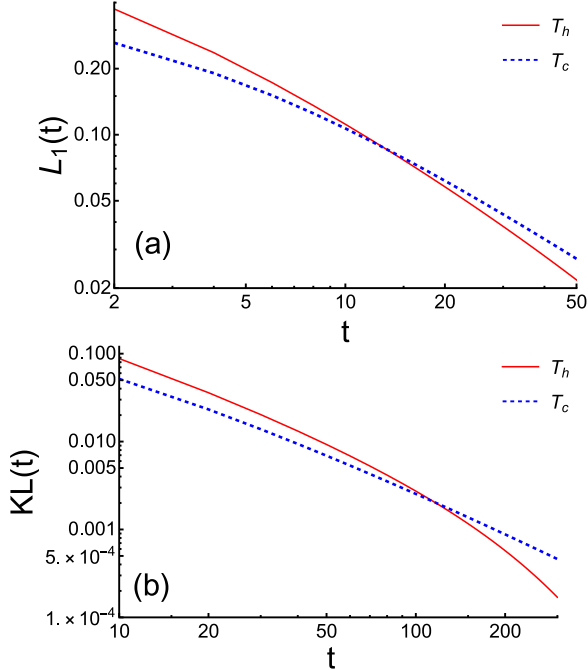


FIG. 3. Illustration of the Mpemba effect in terms of the distance measures: (a) total variation measure (L_1) and (b) Kullback-Leibler (KL) divergence measure. The configuration of the potential is determined by the choice of the parameters: $\alpha = 1.0$, $U_\ell = 4.0$, and $U_r = 10.0$ as considered in Fig. 2(a). The temperatures of the initially hot and cold systems are $T_h = 50$ (solid red) and $T_c = 6$ (dashed blue), respectively. Since the curves cross each other, the Mpemba effect exists.

the inverse Mpemba effect. For the two instances of $U(x)$, shown in Fig. 2(b), $|a_2(T)|$ for $T < 1$ is nonmonotonic for one and monotonic for the other, showing the presence and absence of the inverse Mpemba effect depending on the choice of potential. Beyond showing its existence, we will not discuss the inverse Mpemba effect further.

IV. ROLE OF DISTANCE MEASURES IN THE MPEMBA EFFECT

We now illustrate an example that demonstrates that the existence of the Mpemba effect does not depend on the choice of the distance measures. We consider the potential with parameters as in Fig. 2(a), for which the Mpemba effect, in terms of the criterion based on $|a_2|$, is shown to exist for a wide range of initial temperatures. To show that the Mpemba effect is not dependent on the choice of the criterion, we check whether the effect exists for two choices of distance from steady state: total variation measure, $L_1(t) = \int dx |p(x, t) - \pi(x, T_b)|$, and Kullback-Leibler divergence, $KL(t) = \int dx p(x, t) \ln(p(x, t)/\pi(x, T_b))$. In Fig. 3, we show the variation of these distance measures with time for two different initial conditions relaxing to the same steady state. We note that for these choices of initial conditions, the Mpemba effect exists in terms of $|a_2|$. For both distance measures, we observe a crossing showing that the Mpemba effect exists. The crossing time depends on the choice of the distance measure. This illustrates, through an example, that

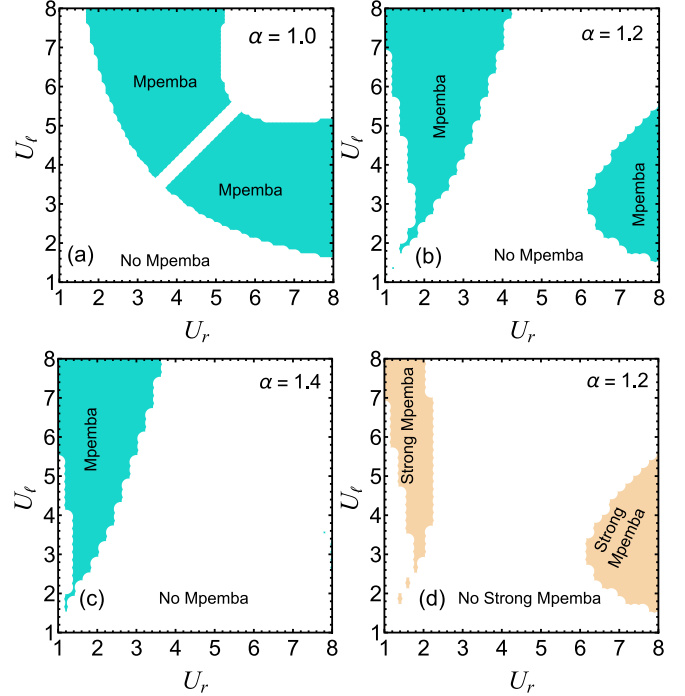


FIG. 4. The U_ℓ - U_r phase diagram showing regions where the Mpemba effect is present (shaded green) and absent (white) for (a) $\alpha = 1.0$, (b) $\alpha = 1.2$, and (c) $\alpha = 1.4$. (d) The U_ℓ - U_r phase diagram showing regions where a strong Mpemba effect is present (shaded yellow) and absent (white) for $\alpha = 1.2$.

the Mpemba effect is independent of the choice of distance measures.

V. PHASE DIAGRAMS

To get an insight into what potentials allow for the Mpemba effect, we now construct phase diagrams demarcating regions that show the Mpemba effect from regions that do not. Note that the potential $U(x)$ is characterized by three parameters: U_ℓ , U_r , and α . Asymmetry in the potential can be introduced through $U_\ell \neq U_r$ and/or $\alpha \neq 1$. The fully symmetric potential is not expected to show the Mpemba effect [26,30]. To explore the effect of all three parameters, we determine the phase diagram in the U_ℓ - U_r plane for fixed α . The phase diagrams for $\alpha = 1.0, 1.2$, and 1.4 are shown in Figs. 4(a)–4(c). First, we observe that, for all three values of α , the fraction of the parameter space that shows the Mpemba effect is not negligible. This implies that, for the single well potential, the Mpemba effect can be observed for generic choices of potentials. Second, we observe that when $U_\ell = U_r$, the Mpemba effect does not exist even if asymmetry is introduced through $\alpha \neq 1$. Thus asymmetry through only different domain widths is not sufficient. Third, when α is increased, thereby increasing asymmetry in the potential, the area of the region showing the Mpemba effect decreases. This is contrary to expectation based on the experiment on colloids [14], where it was observed that asymmetry in domain widths in double well potentials enhanced the Mpemba effect. To further demonstrate that increasing α may not be beneficial, we analyzed the particular case of $U_\ell = 2.0$ and $U_r = 8.0$, and we found

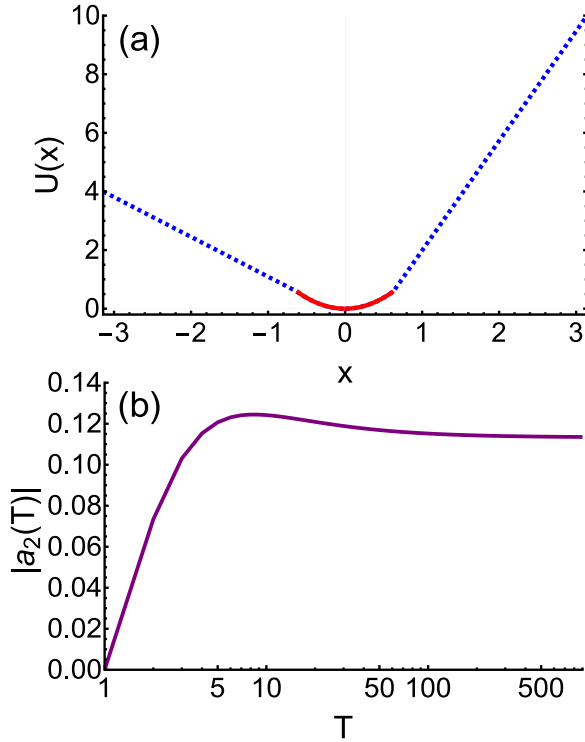


FIG. 5. Numerical results for the illustration of the Mpemba effect for a single well harmonic potential. (a) Shape of the potential with a harmonic well (solid red region) and linear slopes near the boundaries (dashed blue regions). The parameters of the potential are chosen as $\alpha = 1.0$, $-x_{\min} = x_{\max} = \pi$, $k = 1.5$, $U_\ell = 4.0$, $U_r = 10.0$, and $\beta = 0.2$. (b) The variation of $|a_2(T)|$ with temperature T , obtained by a numerical solution, is nonmonotonic, showing the presence of the Mpemba effect.

$$U(x) = \begin{cases} U_\ell + \left(\frac{U_\ell - k(\beta x_{\min})^2}{x_{\min}(1-\beta)}\right)(x - x_{\min}), & x_{\min} < x < \beta x_{\min}, \\ kx^2, & \beta x_{\min} < x < \beta x_{\max}, \\ k(\beta x_{\max})^2 + \frac{U_r - k(\beta x_{\max})^2}{(1-\beta)x_{\max}}(x - \beta x_{\max}), & \beta x_{\max} < x < x_{\max}, \end{cases} \quad (36)$$

where $\beta \in (0, 1)$, and k characterizes the stiffness of the harmonic part of the potential. However, for such potentials, it is no longer possible to analytically solve for the eigenspectrum. Instead, we can solve the eigenspectrum numerically, and thus obtain the coefficient a_2 . For the particular choice of potential, $|a_2(T)|$ is clearly nonmonotonic [see Fig. 5(b)], showing the existence of the Mpemba effect in single well harmonic potentials. Thus, we expect that if the experiment in Ref. [14] is repeated with a single well potential, the Mpemba effect will be observed.

VII. CONCLUSION

In summary, we solved exactly the relaxation dynamics of a Brownian particle in an asymmetric single well potential that is piecewise linear. By identifying the regions in parameter

that the Mpemba effect is present for α only in the domain that is approximately (0.3, 1.1).

We now discuss the existence of a strong Mpemba effect for single well potentials. A strong Mpemba effect refers to the case when the hotter system cools exponentially faster than the colder system. In terms of Eq. (13), this can be achieved only if the coefficient $a_2(T)$ is zero. When $a_2 = 0$, the slowest relaxation mode does not contribute. For $\alpha = 1.2$, we identify those potentials for which a_2 is zero for some temperature. Then, if we choose T_c to be the same temperature, we would observe a strong Mpemba effect. Figure 4(d) shows the phase-space region in the U_ℓ - U_r plane where a strong Mpemba effect is present/absent for $\alpha = 1.2$. Thus, even for the existence of a strong Mpemba effect, a rugged energy landscape is not necessary.

VI. A MORE REALISTIC SETUP

Finally, we discuss the connection to experiments. In the experiment of Kumar and Bechhoefer [14], the Mpemba effect was demonstrated for a colloidal particle trapped in an asymmetric double well harmonic potential with linear behavior near the edges. We now show that the piecewise linear single well potential considered in this paper, when modified to have a harmonic minimum and linear behavior near the edges, continues to exhibit the Mpemba effect. Consider the particular realization of the single well potential, shown in Fig. 5(a), which has a harmonic minimum. The harmonic part is chosen to extend up to βx_{\min} and βx_{\max} . Beyond these cutoffs, $U(x)$ is linear until they meet the boundaries. The potential is described quantitatively as

space that exhibit the Mpemba effect, we not only show that the presence of the Mpemba effect does not require the energy landscape to have multiple minima, but also that the Mpemba effect can be realized for generic choices of potentials. We also demonstrated that both the inverse and strong Mpemba effects can also be realized for single well potentials. We also showed numerically that single well harmonic potentials, as opposed to piecewise linear single well potentials, continue to exhibit the Mpemba effect, opening up the possibility of experimental realization along the lines of the experiment in Ref. [14].

ACKNOWLEDGMENT

We thank S. Vemparala for a critical reading of the manuscript.

- [1] E. B. Mpemba and D. G. Osborne, Cool? *Phys. Ed.* **4**, 172 (1969).
- [2] S. M. Mirabedin and F. Farhadi, Numerical investigation of solidification of single droplets with and without evaporation mechanism, *Int. J. Refrig.* **73**, 219 (2017).
- [3] M. Vynnycky and S. Kimura, Can natural convection alone explain the mpemba effect? *Int. J. Heat Mass Transf.* **80**, 243 (2015).
- [4] J. I. Katz, When hot water freezes before cold, *Am. J. Phys.* **77**, 27 (2009).
- [5] D. Auerbach, Supercooling and the mpemba effect: When hot water freezes quicker than cold, *Am. J. Phys.* **63**, 882 (1995).
- [6] X. Zhang, Y. Huang, Z. Ma, Y. Zhou, J. Zhou, W. Zheng, Q. Jiang, and C. Q. Sun, Hydrogen-bond memory and water-skin supersolidity resolving the mpemba paradox, *Phys. Chem. Chem. Phys.* **16**, 22995 (2014).
- [7] Y. Tao, W. Zou, J. Jia, W. Li, and D. Cremer, Different ways of hydrogen bonding in water - why does warm water freeze faster than cold water?, *J. Chem. Theor. Comput.* **13**, 55 (2017).
- [8] J. Jin and W. A. Goddard III, Mechanisms underlying the mpemba effect in molecular dynamics simulations, *J. Phys. Chem. C* **119**, 2622 (2015).
- [9] A. Gijón, A. Lasanta, and E. R. Hernández, Paths towards equilibrium in molecular systems: The case of water, *Phys. Rev. E* **100**, 032103 (2019).
- [10] H. C. Burridge and P. F. Linden, Questioning the mpemba effect: hot water does not cool more quickly than cold, *Sci. Rep.* **6**, 37665 (2016).
- [11] P. Chaddah, S. Dash, K. Kumar, and A. Banerjee, Overtaking while approaching equilibrium, [arXiv:1011.3598](https://arxiv.org/abs/1011.3598).
- [12] C. Hu, J. Li, S. Huang, H. Li, C. Luo, J. Chen, S. Jiang, and L. An, Conformation directed mpemba effect on polylactide crystallization, *Cryst. Growth Des.* **18**, 5757 (2018).
- [13] Y.-H. Ahn, H. Kang, D.-Y. Koh, and H. Lee, Experimental verifications of mpemba-like behaviors of clathrate hydrates, *Korean J. Chem. Eng.* **33**, 1903 (2016).
- [14] A. Kumar and J. Bechhoefer, Exponentially faster cooling in a colloidal system, *Nature (London)* **584**, 64 (2020).
- [15] A. Kumar, R. Chétrite, and J. Bechhoefer, Anomalous heating in a colloidal system, *Proc. Natl. Acad. Sci. (USA)* **119**, e2118484119 (2022).
- [16] J. Bechhoefer, A. Kumar, and R. Chétrite, A fresh understanding of the Mpemba effect, *Nat. Rev. Phys.* **3**, 534 (2021).
- [17] M. Ibáñez, C. Dieball, A. Lasanta, A. Godec, and R. A. Rica, Heating and cooling are fundamentally asymmetric and evolve along distinct pathways, [arXiv:2302.09061](https://arxiv.org/abs/2302.09061).
- [18] A. Gal and O. Raz, Precooling Strategy Allows Exponentially Faster Heating, *Phys. Rev. Lett.* **124**, 060602 (2020).
- [19] I. Klich, O. Raz, O. Hirschberg, and M. Vucelja, Mpemba Index and Anomalous Relaxation, *Phys. Rev. X* **9**, 021060 (2019).
- [20] I. Klich and M. Vucelja, Solution of the metropolis dynamics on a complete graph with application to the markov chain mpemba effect, [arXiv:1812.11962](https://arxiv.org/abs/1812.11962).
- [21] N. Vadakkayil and S. K. Das, Should a hotter paramagnet transform quicker to a ferromagnet? Monte Carlo simulation results for Ising model, *Phys. Chem. Chem. Phys.* **23**, 11186 (2021).
- [22] I. González-Adalid Pemartín, E. Mompó, A. Lasanta, V. Martín-Mayor, and J. Salas, Slow growth of magnetic domains helps fast evolution routes for out-of-equilibrium dynamics, *Phys. Rev. E* **104**, 044114 (2021).
- [23] G. Teza, R. Yaacoby, and O. Raz, Relaxation Shortcuts through Boundary Coupling, *Phys. Rev. Lett.* **131**, 017101 (2023).
- [24] Z. Lu and O. Raz, Nonequilibrium thermodynamics of the markovian mpemba effect and its inverse, *Proc. Natl. Acad. Sci. (USA)* **114**, 5083 (2017).
- [25] T. Van Vu and Y. Hasegawa, Toward relaxation asymmetry: Heating is faster than cooling, *Phys. Rev. Res.* **3**, 043160 (2021).
- [26] M. R. Walker and M. Vucelja, Anomalous thermal relaxation of langevin particles in a piecewise-constant potential, *J. Stat. Mech.: Theor. Expt.* (2021) 113105.
- [27] D. M. Busiello, D. Gupta, and A. Maritan, Inducing and optimizing markovian mpemba effect with stochastic reset, *New J. Phys.* **23**, 103012 (2021).
- [28] A. Lapolla and A. Godec, Faster Uphill Relaxation in Thermodynamically Equidistant Temperature Quenches, *Phys. Rev. Lett.* **125**, 110602 (2020).
- [29] M. R. Walker and M. Vucelja, Mpemba effect in terms of mean first passage times of overdamped langevin dynamics on a double-well potential, [arXiv:2212.07496](https://arxiv.org/abs/2212.07496).
- [30] J. Degünther and U. Seifert, Anomalous relaxation from a non-equilibrium steady state: An isothermal analog of the mpemba effect, *Europhys. Lett.* **139**, 41002 (2022).
- [31] F. J. Schwarzendahl and H. Löwen, Anomalous Cooling and Overcooling of Active Colloids, *Phys. Rev. Lett.* **129**, 138002 (2022).
- [32] M. Baity-Jesi, E. Calore, A. Cruz, L. A. Fernandez, J. M. Gil-Narvió, A. Gordillo-Guerrero, D. Iñiguez, A. Lasanta, A. Maiorano, E. Marinari *et al.*, The mpemba effect in spin glasses is a persistent memory effect, *Proc. Natl. Acad. Sci. (USA)* **116**, 15350 (2019).
- [33] A. Santos and A. Prados, Mpemba effect in molecular gases under nonlinear drag, *Phys. Fluids* **32**, 072010 (2020).
- [34] R. Gómez González, N. Khalil, and V. Garzó, Mpemba-like effect in driven binary mixtures, *Phys. Fluids* **33**, 053301 (2021).
- [35] R. G. González and V. Garzó, Anomalous mpemba effect in binary molecular suspensions, *EPJ Web Conf.* **249**, 09005 (2021).
- [36] A. Patrón, B. Sánchez-Rey, and A. Prados, Strong nonexponential relaxation and memory effects in a fluid with nonlinear drag, *Phys. Rev. E* **104**, 064127 (2021).
- [37] F. Carollo, A. Lasanta, and I. Lesanovsky, Exponentially Accelerated Approach to Stationarity in Markovian Open Quantum Systems through the Mpemba Effect, *Phys. Rev. Lett.* **127**, 060401 (2021).
- [38] A. K. Chatterjee, S. Takada, and H. Hayakawa, Quantum mpemba effect in a quantum dot with reservoirs, [arXiv:2304.02411](https://arxiv.org/abs/2304.02411).
- [39] A. Nava and M. Fabrizio, Lindblad dissipative dynamics in the presence of phase coexistence, *Phys. Rev. B* **100**, 125102 (2019).
- [40] R. Holtzman and O. Raz, Landau theory for the mpemba effect through phase transitions, *Commun. Phys.* **5**, 280 (2022).
- [41] S. Zhang and J.-X. Hou, Theoretical model for the mpemba effect through the canonical first-order phase transition, *Phys. Rev. E* **106**, 034131 (2022).
- [42] G. Teza, R. Yaacoby, and O. Raz, Eigenvalue Crossing as a Phase Transition in Relaxation Dynamics, *Phys. Rev. Lett.* **130**, 207103 (2023).

- [43] A. Lasanta, F. Vega Reyes, A. Prados, and A. Santos, When the Hotter Cools More Quickly: Mpemba Effect in Granular Fluids, *Phys. Rev. Lett.* **119**, 148001 (2017).
- [44] A. Torrente, M. A. López-Castaño, A. Lasanta, F. V. Reyes, A. Prados, and A. Santos, Large mpemba-like effect in a gas of inelastic rough hard spheres, *Phys. Rev. E* **99**, 060901(R) (2019).
- [45] E. Mompó, M. A. López-Castaño, A. Lasanta, F. Vega Reyes, and A. Torrente, Memory effects in a gas of viscoelastic particles, *Phys. Fluids* **33**, 062005 (2021).
- [46] A. Biswas, V. V. Prasad, O. Raz, and R. Rajesh, Mpemba effect in driven granular Maxwell gases, *Phys. Rev. E* **102**, 012906 (2020).
- [47] A. Biswas, V. V. Prasad, and R. Rajesh, Mpemba effect in an anisotropically driven granular gas, *Europhys. Lett.* **136**, 46001 (2021).
- [48] A. Biswas, V. Prasad, and R. Rajesh, Mpemba effect in anisotropically driven inelastic maxwell gases, *J. Stat. Phys.* **186**, 45 (2022).
- [49] A. Megías and A. Santos, Mpemba-like effect protocol for granular gases of inelastic and rough hard disks, *Front. Phys.* **10**, 971671 (2022).
- [50] A. Biswas, V. V. Prasad, and R. Rajesh, Mpemba effect in driven granular gases: Role of distance measures, *Phys. Rev. E* **108**, 024902 (2023).
- [51] S. S. Chittari and Z. Lu, Geometric approach to nonequilibrium hasty shortcuts, [arXiv:2304.06822](https://arxiv.org/abs/2304.06822).
- [52] A. Biswas, R. Rajesh, and A. Pal, Mpemba effect in a Langevin system: Population statistics, metastability, and other exact results, *J. Chem. Phys.* **159**, 044120 (2023).
- [53] H. Risken, Fokker-planck equation, in *The Fokker-Planck Equation* (Springer, Berlin, Heidelberg, 1996), pp. 63–95.
- [54] M. Mörsch, H. Risken, and H. Vollmer, One-dimensional diffusion in soluble model potentials, *Z. Phys. B* **32**, 245 (1979).
- [55] V. Ledoux, M. Van Daele, and G. V. Berghe, Efficient computation of high index Sturm-Liouville eigenvalues for problems in physics, *Comput. Phys. Commun.* **180**, 241 (2009).